Communications to the Editor

Form Factor of Salt-Free Linear Polyelectrolytes

Mark J. Stevens*,† and Kurt Kremer

Institut für Festkörperforschung, Forschungszentrum Jülich, Postfach 1913, D-52425 Jülich, Federal Republic of Germany

Received March 16, 1993
Revised Manuscript Received June 5, 1993

In contrast to our rather good understanding of the structure of neutral polymers,[1] charged polymers have been a source of mystery.[2-5] This lack of understanding continues even though much research has been performed[4,5] on both biological polyelectrolytes (e.g., RNA, DNA) and synthetic polyelectrolytes (e.g., NaPSS). Theoretically, difficulties of the long-ranged Coulomb interaction have stymied progress. Experiments have observed interesting phenomena but have not been able to definitively characterize the chain structure.[4-6] The inherent complications of studying polyelectrolytes suggest a strong need for simulation studies that examine their structure. We report here results of molecular dynamics simulations on a prototypical *system* of many polymers with every monomer charged and no added salt. This is an idealization of the typical practical situation where not all monomer units are charged and the solvent has a finite ionic strength. However, because the fully charged, no salt case is the limiting structure where the Coulomb interactions play the central role, it merits deep understanding.

The basic effect of charges on a polymer is the chain expansion due to the Coulomb repulsion. In the infinite chain length and dilute concentration limit, the chains are expected to be stretched like a rod.[7] Increasing polymer concentration results in a screening of the Coulomb interaction which reduces the amount of stretching. The nature of this stretching can only be calculated for weakly interacting systems.[8,9] Most theories assume screened Coulomb or Debye–Hückel interactions. Starting with Odijk,[10] various pictures of the polyelectrolyte chain structure have been suggested based on the results for the persistence length, L_p, the length over which the chain is "straight".[11,12] The basic picture has the chains as rods at very dilute concentrations. The rods begin to bend at the concentration at which the chain length, L, equals the persistence length. Further transitions occur at higher concentrations, in particular at the concentration in the semidilute regime where the strand–strand distance equals the persistence length. At sufficiently high concentrations the Coulomb interactions are effectively screened out and the polyelectrolytes are expected to be Gaussian chains.

In this paper we focus on the chain form factor or single-chain structure factor, $S(q)$, a convenient way to describe the single-chain structure, as a function of monomer density ranging from very dilute to semidilute. Moreover, $S(q)$ is the usual quantity that is experimentally measured to determine polymer structure. Unfortunately, this is difficult to determine experimentally.[4]

In contrast to all previous simulations,[13] we consider a system of several (8–32) chains instead of just a single chain. This allows us for the first time to examine polyelectrolyte structure from the dilute into the semidilute regime. This concentration variation is essential for several reasons. Since charged polymers are stretched in comparison with neutral polymers, the monomer overlap concentration, ρ_m^*, is at much lower values. This, coupled with the need for a sufficiently strong signal, results in almost all experiments being performed at semidilute concentrations. Moreover, even though the chains may not overlap, they can still interact through the long-range Coulomb potential, making consideration of interchain interactions essential even far below ρ_m^*. None of the previous simulations[13] is able to take into account the fluctuations caused by the complex chain–counterion–chain interactions.

The details of our simulations follow the successful methods used in neutral polymer simulations.[14,15] The system studied is composed of several bead–chain polymers with monovalent monomers in a salt-free solution with the counterions treated explicitly. This model corresponds to flexible polyelectrolytes like RNA and NaPSS. Simulations were done on systems of 8 or 16 chains composed of (N_b =) 16, 32, and 64 beads. A few runs of 4 chains with 128 beads were also done to further test chain-length dependence, and one run of 32 chains of 32 beads was done to test number dependence. The bond potential is the FENE (nonlinear spring) potential with spring constant $k = 7\epsilon/\sigma^2$ and maximum extent $R_0 = 2\sigma$, where here as throughout the letter Lennard-Jones (LJ) units are used.[15] The average bond length is 1.1σ. A repulsive LJ interaction with a cutoff of $2^{1/6}\sigma$ produces excluded volume for monomer–monomer and monomer–counterion interactions. For counterion–counterion interactions the LJ cutoff is $2^{1/6}\sigma/4$.

The Coulomb interactions are evaluated by a spherical approximation to the Ewald sum given by Adams and Dubey.[16] This is an order of magnitude better than the minimum image method which is the best that has been done albeit only for simulations of a single chain.[13] The Coulomb coupling is given by the Bjerrum length, λ_B, which for our simulations is 0.9 times the average bond length, b; thus, we are close to the Manning condensation transition point and in the strong interaction regime. For one run we have checked that the results of this approximate form are consistent with a more accurate Kubic harmonic expansion of order 8. In both cases a truncated octahedral cell is used as it provides better convergence than a simple cube.

The dynamics of the system is done at constant temperature, $T = 1.2\epsilon$, using the Langevin thermostat with damping constant $\Gamma = \tau^{-1}$ and timestep 0.015τ.[14,15] The solvent is included via the damping of the Langevin thermostat which produces Rouse dynamics and via the dielectric constant within λ_B. The simulations times are such that the chain center of mass moves at least 10 times

† Present address: Corporate Research Science Laboratories, Exxon Research and Engineering Co., Annandale, NJ 08801.

0024-9297/93/2226-4717$04.00/0

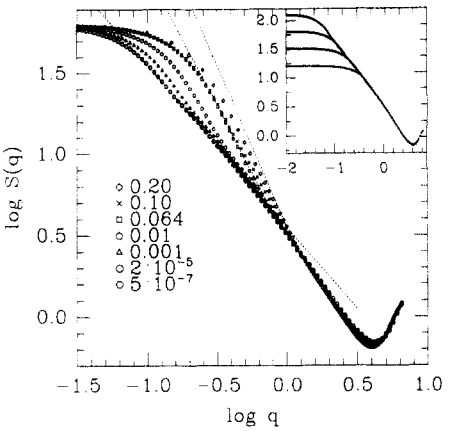

Figure 1. Form factor for 64 beads chains gradually changing from apparent rodlike to coiled form with increasing monomer density. This contradicts the theoretically expected form which is a combination of rigid-rod, good solvent chain, and ideal chain forms. The dotted lines give slopes of −1, $-5/3$, and −2 which correspond to the q dependence of a rigid rod, good solvent chain, and ideal chain. For $0 < \log q\sigma < 0.2$ the slope is greater than 1, implying the chains are not fully stretched in this regime. The inset shows the chain-length independence at $q > 2\pi/R$ at $\rho_m = 0.001\sigma^{-3}$ for N_b = 16, 32, 64, and 128.

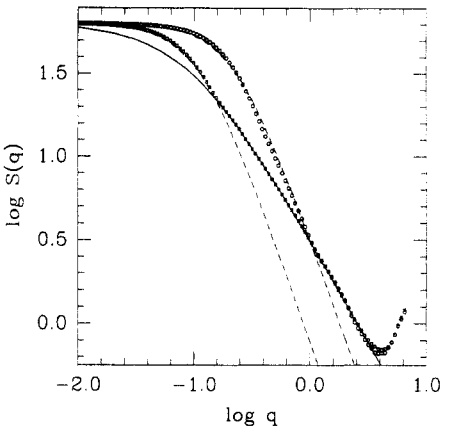

Figure 2. Form factors at $\rho_m = 2 \times 10^{-5}$ and 0.1 fitted by a combination of two Debye functions (see text for form). The solid (dashed) line represents the Debye function with $\nu = 0.80$ ($\nu = 1/2$). The dip in $S(q)$ occurs at the intersection of the two fits.

the chain contour length. For 64 bead chains this required about 10^6 timesteps.

We define the chain form factor as

$$S(\mathbf{q}) = \frac{1}{N_b}\left|\sum_{j=1}^{N_b} \exp(i\mathbf{q}\cdot\mathbf{r}_j)\right|^2 \qquad (1)$$

where the normalization is $S(0) = N_b$, and we calculate the spherically averaged quantity, $S(q)$. In the range $2\pi/R < q < 2\pi/b$, where R is the average end-to-end distance and b is the bond length, $S(q)$ scales as $q^{-1/\nu}$ for neutral polymers with $R \sim N_b^{\nu}$.[1] The ideal chain and good solvent chain values of ν are $1/2$ and 0.588 ($\approx 3/5$), respectively. Scaling predictions for $S(q)$ have been based on the picture that the polyelectrolyte's structure is composed of rodlike segments which together form an ideal chain.[3,7,10] For wavevectors greater than the inverse segment length, or persistence length, L_p,[8,9] the form factor should scale as $1/q$. For $q < 2\pi/L_p$, the ideal chain would yield $\nu = 1/2$. However, we have good solvent chains and should see $\nu \approx 3/5$ at dilute densities and $\nu = 1/2$ for semidilute and dense solutions.

We show our calculated $S(q)$ spanning dilute and semidilute ranges for the 64 bead chains in Figure 1. For this chain length the crossover monomer density, $\rho_m^* = (\pi R^3/6)^{-1}$, is approximately $0.017\sigma^{-3}$. The slopes of the curves in Figure 1 give $-1/\nu$, and the dotted lines starting from the top left of the figure have slopes of −1, $-5/3$, and −2. The form factors show no chain-length dependence for $q \gtrsim 2\pi/R$ as shown in the inset for $\rho_m = 0.001$. Within this range of q end effects are not important and we can consider the results for $N_b = 64$ to be valid for longer chains. From Figure 1 we see that below the monomer density, $\rho_m = 2 \times 10^{-5}$, the form factor is unchanged. This saturation occurs at a characteristic chain-length-dependent density and is discussed elsewhere.[17] At this density the average counterion spacing ($\rho_m^{-1/3}$) roughly equals the chain length. A further reduction in the density does not further reduce the screening by the counterions.

A density-independent regime occurs at relatively high wavevectors ($1 \lesssim q\sigma \lesssim 2\pi/2$) which corresponds to short length scales up to about 6 bond lengths. The density-independent behavior below q_0 ($\approx\sigma^{-1}$) and the change in slope at q_0 suggest the existence of stretched blobs,[7] whose lengths are about $6b$. The nature of these blobs is quite surprising. In the high q region the slope is *not* −1 as expected when $q > 2\pi/L_p$. Instead, we find a fixed value *independent of density and chain length* as long as the strand–strand distance exceeds $2\pi/q_0$. The structure on short length scales certainly does not correspond to any of the theoretical pictures.[7-9]

To better see the scaling of the form factor in the dilute regime, one can analyze $q^{1/\nu}S(q)$. We find that, for $1 < q\sigma < 2\pi/2$, $\nu = 0.80$ gives the best scaling. Thus, the chains are stretched beyond the neutral good solvent value, but well below the rod value. On the other hand, the chains are stretched even more on longer length scales at low density. At $q = q_0$ a crossover occurs to $\nu \simeq 0.90$. Attributing a single value to the scaling is approximate, since the exponent ν varies continuously. However, one can definitely distinguish the structures (i.e., scaling exponents) below and above q_0. Furthermore, it is clear that $\nu = 1$ does not fit the data in any regime of the present systems.

At small wavevectors the scaling of the form factor shows a pronounced density dependence. The slopes in Figure 1 at low q ($q \lesssim \sigma^{-1}$) vary continuously from 0.9 to about the good solvent value, 0.6, with increasing ρ_m. The good solvent value of ν is reached at $\rho_m = 0.064\sigma^{-3}$, a density well above the overlap density. Eventually at higher density the neutral chain limit must be reached. At ρ_m^* we find that $\nu = 0.80$ extends to below q_0. Thus, the transition between being stretched most at long or short length scales occurs at ρ_m^*. The continuous variation in ν contrasts with the picture of just two values of ν. Evidently, not only the length over which the Coulomb interaction stretches the chain but also the degree of stretching depend on the screening.

Our calculated form factors have a simple form and we can fit our data rather well by a suitable generalization of the Debye form factor of an ideal neutral chain:

$$S_D(q) = N_b/(1 + (qa)^{1/\nu_D}) \qquad (2)$$

where a and ν_D are fit parameters ($\nu_D = 1/2$ and $a = R_g/\sqrt{2}$ are the ideal chain values). This form satisifies the normalization and gives the expected form, $S_D(q) \sim q^{-1/\nu_D}$, when $(qa)^{1/\nu_D} \gg 1$. The parameters ν_D and a can be determined from the values of the calculated $S(q)$ and $dS(q)/dq$ at some q. We can fit the calculated $S(q)$ for $q \lesssim 2\pi/2\sigma$ with two Debye functions, thus providing a simple parametrization (Figure 2). The changeover from one fit

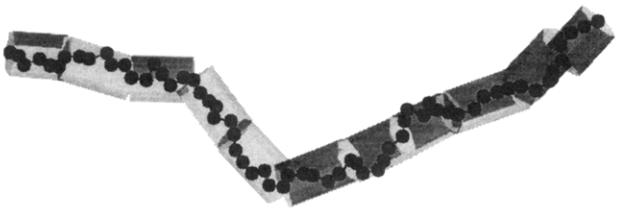

Figure 3. Our picture of linear polyelectrolytes depicted showing a tube surrounding the chain ($\rho_m = 0.001\sigma^{-3}$). The tube is made of straight tubelets of length approximately $6b$ in which the chain is stretched beyond the good solvent structure. The overall tube is stretched to a degree depending on the density.

function to the other occurs at a dip, at $q = q_d$, apparent in the form factor. For $\rho_m < \rho_m^*$, $q_d \approx 2\pi/R$. The slopes in the high and low q-regimes are equal at ρ_m^* and above the overlap density, q_d decreases faster than $2\pi/R$, now governed by the strand–strand distance.

In the high q region ($q > q_d$) we find that ν_D is independent of density for a given chain length. Figure 2 shows that the high q fit works at both low and high densities. At $\rho_m < \rho_m^*$ this fit extends to $q < q_0$. We can extrapolate the structure of longer chains by fitting the 64 bead chain data at $q > 2\pi/R$ with S_D but with a larger N_b. From this extrapolation we can say that, for $\rho_m = 2 \times 10^{-5}$, the chain structure never becomes rodlike ($S(q) \sim 1/q$) for any N_b.

Given that we find no chain-length dependence at a given density, the only possibility for rodlike structure is at lower density and longer chains. If we use the value of the Bjerrum length in water, $\lambda_B = 7.14$ Å, to set the length scale, then $\rho_m = 2 \times 10^{-5} = 9 \times 10^{-5}$ monomol/L. This is a very low density, suggesting that, for physically realizable flexible polyelectrolytes, the rodlike structure will not be seen for experimentally realizable densities. These results are consistent with recent experiments.[18,19]

The low-q fits are not particularly revealing beyond showing that a simple form can describe the data. In order to be consistent with the small q limit to second order in q, we fix $\nu_D = {}^1/_2$ for the low-q fits at all densities and fit a. While better fits could be obtained by varying ν_D, this constraint yields fits as good as the Debye fit for neutral polymers and satisfies an important criterion. Since $\nu_D \neq \nu$, the value of ${}^1/_2$ does not imply a Gaussian structure. The degree of bending is best described in terms of the varying slopes as discussed above.

We can summarize our results in a new picture (Figure 3) for the structure of linear polyelectrolytes. The chain is composed of short segments that are stretched by the Coulomb repulsion but are not rodlike. The size of these segments will most likely be dependent on the intrinsic chain stiffness and the Coulomb strength, but they seem independent of chain length and density. The occurrence of these high q fluctuations can be rationalized by estimating the free energy of small kinks in the chain. The entropy of such a kink as well as the upper limit of the energy of the excitation scales as $k_BT \ln L$. Thus, one should expect that such high q fluctuations will eventually cause the short length scale exponent to be 0.8 instead of 1. The chain composed of these segments has a structure that is density dependent. At very dilute concentrations, the segment chain is straighter than the segments but not rodlike. There still occur strong fluctuations leading to horseshoe-shaped configurations. These low q deformations are directly related to charge density fluctuations of the counterions. With increasing concentration, the Coulomb interactions between segments become more screened and the chain of segments becomes increasingly bent. At a length scale proportional to the Debye length, the chains become more bent than the segments.

Acknowledgment. We thank P. A. Pincus for very useful discussions. The simulations were made possible by a grant from the Höchstleistungsrechenzentrum, Germany, within the Disordered Polymers Project. A NATO Travel Grant is also acknowledged.

References and Notes

(1) de Gennes, P.-G. *Scaling Concepts in Polymer Physics*; Cornell University Press: Ithaca, NY, 1979.
(2) Cates, M. *J. Phys. II Fr.* **1992**, *2*, 1109.
(3) Hayter, J.; Jannink, G.; Brochard-Wyart, F.; de Gennes, P.-G. *J. Phys. Lett.* **1980**, *41*, 451.
(4) Jannink, G. *Makromol. Chem., Macromol. Symp.* **1986**, *1*, 67.
(5) Schurr, J.; Schmitz, K. *Annu. Rev. Phys. Chem.* **1986**, *37*, 271.
(6) Wang, L.; Bloomfield, V. *Macromolecules* **1990**, *23*, 804.
(7) de Gennes, P.-.G.; Pincus, P.; Velasco, R.; Brochard, F. *J. Phys. (Paris)* **1976**, *37*, 1461.
(8) Odijk, T. *J. Polym. Sci., Polym. Phys. Ed.* **1977**, *15*, 477.
(9) Skolnick, J.; Fixman, M. *Macromolecules* **1977**, *10*, 944.
(10) Odijk, T. *Macromolecules* **1979**, *12*, 688.
(11) Weill, G. *J. Phys. (Paris)* **1988**, *49*, 1049.
(12) Kaji, K.; Urakawa, J.; Kanaya, T.; Kitamaru, R. *J. Phys. (Paris)* **1988**, *49*, 993.
(13) Christos, G. A.; Carnie, S. L. *J. Chem. Phys.* **1989**, *91*, 439. Reed, C.; Reed. W. *J. Chem. Phys.* **1990**, *92*, 6916. Brender, C.; Danino, M. *J. Chem. Phys.* **1992**, *97*, 2119. Barrat, J. L.; Boyer, D. *J. Phys. II Fr.* **1993**, *3*, 343. See also references therein.
(14) Kremer, K.; Grest, G. *J. Chem. Phys.* **1990**, *92*, 5057.
(15) Dünweg, B.; Kremer, K. *Phys. Rev. Lett.* **1982**, *66*, 2996.
(16) Adams, D.; Dubey, G. *J. Comput. Phys.* **1987**, *72*, 156.
(17) Stevens, M.; Kremer, K., to be published.
(18) Degiorgio, V.; Mantegazza, F.; Piazza, R. *Europhys. Lett.* **1991**, *15*, 75.
(19) Schmidt, M. *Macromolecules* **1991**, *24*, 5361.